Biosensors and Bioelectronics 91 (2017) 183–189

Contents lists available at ScienceDirect

Biosensors and Bioelectronics

journal homepage: www.elsevier.com/locate/bios

Ultrasensitive electrochemical DNA biosensor based on functionalized gold clusters/graphene nanohybrids coupling with exonuclease III-aided cascade target recycling

Wei Wang[1], Ting Bao[1], Xi Zeng, Huayu Xiong, Wei Wen, Xiuhua Zhang, Shengfu Wang*

Hubei Collaborative Innovation Center for Advanced Organic Chemical Materials, Ministry of Education Key Laboratory for the Synthesis and Application of Organic Functional Molecules & College of Chemistry and Chemical Engineering, Hubei University, Wuhan 430062, PR China

ARTICLE INFO

Keywords:
Electrochemical biosensor
Target DNA
AuNCs/GR nanohybrids
Exonuclease III-aided cascade target recycling
Enzyme-catalyzed silver deposition

ABSTRACT

In this work, a novel and ultrasensitive electrochemical biosensor was constructed for DNA detection based on functionalized gold clusters/graphene nanohybrids (AuNCs/GR nanobybrids) and exonuclease III (Exo III)-aided cascade target recycling. By utilizing the capacity of GR as universal template, different metal nanoclusters including AuNCs/GR nanobybrids and PtNCs/GR nanohybrids were synthesized through convenient ultrasonic method. Exo III-aided cascade recycling was initiated by target DNA, generating the final cleavage product (S2), which acted as a linkage between capture probe and the functionalized metal nanoclusters/GR conjugates in the construction of the biosensor. The AuNCs/GR-DNA-enzyme conjugates acted as interfaces of enzyme-catalyzed silver deposition reaction, achieving DNA detection ranging from 0.02 fM to 20 pM with a detection limit of 0.057 fM. In addition, PtNCs/GR-DNA conjugates presented peroxidase-like activity and the functionalized PtNCs/GR nanohybrids-based electrochemical biosensor also realized DNA detection by catalyzing the 3,3′,5,5′-tetramethylbenzidine-hydrogen peroxide (TMB-H_2O_2) system to produce electrochemical signal. This metal clusters/GR-based multiple-amplified electrochemical biosensor provided an universal method for DNA detection.

1. Introduction

Nucleic acids are vital genetic material in cell nucleus which contain the instructions of genetic information. Besides, they are featured in protein biosynthesis, playing a decisive role in a series of major life process including growth, heredity and variation (Chargaff, 1951). Due to such a supernormal role, nucleic acids are specific biomarkers involved in many pressing diseases. Gene damage and gene mutation cause familial hereditary disease and intractable disease with high risk, for instance, myotonic muscular dystrophy, hemophilia, inflammatory bowel and tumour (Fu et al., 1992; Holzer, 1998; Kaghad et al., 1997; Levinson et al., 1987). Therefore, detection of trace amount of specific-sequence DNA is of hugely important in the early diagnosis of gene-related diseases, which is of signality in biomedical research and clinical diagnosis (Rosi et al., 2006; Zhang et al., 2013).

Detection methods for DNA include fluorescence (Zuo et al., 2010; Ye et al., 2016), surface-enhanced Raman scattering (SERS) (Ngo et al., 2016; Zeng et al., 2016), colorimetry (Liu et al., 2013; Yun et al., 2016) and electrochemical biosensor (Tan et al., 2015; Wang et al., 2016). There into, electrochemical biosensor based on diversified signal amplification strategies is an effective and sensitive tool for DNA detection (Gerasimova and Kolpashchikov, 2014; Zhao et al., 2015). In the construction of electrochemical biosensor, enzyme-catalyzed reaction and exonuclease (Exo)-aided target recycling have been widely used for signal enhancement, which improve the sensitivity of bioassays (Liu et al., 2016; Wang et al., 2015). In enzyme-catalyzed reaction, frequently-used enzymes are horse radish peroxidase (HRP), peroxidase, glucose oxidase (GOD) and alkaline phosphatase (ALP). Compared with other enzymes, ALP is arrestive for its activity in biocatalytic metal deposition reaction. In ALP-catalyzed silver deposition reaction, ascorbic acid 2-phosphate (AAP) is traditionally used as catalytic substrate, the generated ascorbic acid (AA) acts as reducing agent for Ag^+, the reduced Ag nanoparticles (AgNPs) finally deposited on the surface of ALP (Basnar et al., 2006; Feng et al., 2011). As to the Exo-aided target recycling, the presence of target initiates the cleavage process, the hydrolysis occurs upon target binding, followed with the releasing of target. Commonly used Exos are Exo I, RecJf, Exo III and λ-exo. Among them, Exo III is effective on 3′-terminal of double-

* Corresponding author.
E-mail address: wangsf@hubu.edu.cn (S. Wang).
[1] W. Wang and T. Bao contributed equally to this work.

http://dx.doi.org/10.1016/j.bios.2016.12.017
Received 1 September 2016; Received in revised form 5 December 2016; Accepted 7 December 2016
Available online 10 December 2016
0956-5663/

stranded DNA, thus we can flexibly utilize the cleavage property of Exo III to obtain a certain DNA sequence via appropriate design (Bao et al., 2015; Zhang et al., 2011).

Gold nanoclusters (AuNCs) are gold nanomaterial composed of several to few hundreds of Au atoms with ultra-small sizes commensurate to the Fermi wavelength of electrons. For the size-specific properties, AuNCs present distinctly different optical and chemical properties, which have attracted considerable attention and been widely used in many fields including fluorescence, photoluminescence and catalytic reactivity (Jin, 2015). So far, many methods have been applied to synthesize AuNCs. For example, thiolated compounds are used to reduce chloroauric acid to synthesize AuNCs, such as dithiothreitol, mercaptoundecanoic acid and 8-Mercapto-9-propyladenine (Ding et al., 2014; Sun et al., 2014; Venkatesh et al., 2014). Proteins also have been used as template to prepare AuNCs, including glutathione, trypsin and bovine serum albumin (BSA) (Farrag et al., 2013; Chang and Ho, 2015; Shamsipur et al., 2015). AuNCs also can be synthesized by the reductive effect of dimethylformamide (DMF) (Liu et al., 2008; Kawasaki et al., 2010). Besides, graphene (GR) can be used as template to synthesize AuNCs and obtain the AuNCs/GR nanohybrids (Yin et al., 2012). Compared with other methods, the GR-based method has short synthesis period without addition of protecting protein or reducing agent, which is very clean and simple. Morever, GR has incomparable conductibility compared with other templates including thiolated compounds and proteins. As to the AuNCs/GR nanohybrids, the conductive GR sheets act as effective mediator of the metal-support interaction, on which AuNCs distributed uniformly. Owing to the excellent conductivity of GR and AuNCs, the AuNCs/GR nanohybrids have promising potential in the construction of biosensing interfaces. Many DNA biosensors based on various nanomaterials and amplification strategies have been reported previously, including nitrogen-doped GR/Au nanoparticles, GR/Au nanorod/polythionine, DNAzyme amplification and Exo III-assisted cascade signal amplification (Chen et al., 2016; Huang et al., 2015; Liu et al., 2015; Xiong et al., 2017). However, they were limited by the complex synthetic procedures, expensive instrument or the low sensitivity. Compared with these reported biosensors, the superiority of the proposed biosensor was utilizing the GR as an universal template to synthesize different metal nanoclusters including AuNCs/GR and PtNCs/GR nanohybrids, which was very simple and convenient, and different catalytic interfaces and catalytic reactions were successfully constructed. The combination of several attractive amplification strategies including AuNCs/GR nanohybrids, Exo III-aided cascade target recycling and enzyme-catalyzed reaction improved the sensitivity significantly. Up to now, related research of AuNCs/GR nanohybrids-based functionalized catalytic interfaces coupling with Exo III-aided cascade target recycling for DNA recognition has not been reported.

Herein, we developed a multiple-amplified electrochemical biosensor for DNA detection based on functionalized AuNCs/GR nanohybrids and Exo III-aided cascade target recycling for signal amplification. Target DNA triggered the Exo III-aided cascade target recycling process which generated the final cleavage product (S2). With the presence of S2, the electrochemical biosensor was successfully constructed with the functionalized AuNCs/GR nanohybrids performing as the interfaces of enzyme-catalyzed silver deposition reaction. The proposed biosensor realized ultrasensitive DNA detection and could specifically distinguish target DNA from mismatched DNA. This strategy provided a versatile tool that had great potential for DNA detection in bio-analysis.

2. Experimental section

2.1. Materials and reagents

Gold (III) chloride trihydrate ($HAuCl_4 \cdot 3H_2O$), silver nitrate ($AgNO_3$) and ALP were purchased from Sigma-Aldrich co. (St. Louis, USA). Ammonia solution, chloroplatinic acid hexahydrate ($H_2PtCl_6 \cdot 6H_2O$), tris(2-carboxyethyl) phosphine hydrochloride (TCEP), cetyltrimethylammonium bromide (CTAB), albumin from bovine serum (BSA), glycine, sodium borohydride ($NaBH_4$), hydrogen peroxide (H_2O_2) and 3,3′,5,5′-tetramethylbenzidine (TMB) were received from Aladdin Bio-Chem Technology Co., Ltd. (Shanghai, China). AAP was got from DiBai Chemical Technology co., Ltd. (Shanghai, China). All solutions used in the experiment were prepared using ultrapure water (resistivity of 18.25 MΩ cm) from Aquapro water purification system. All oligonucleotides were synthesized and purified by Sangon Biotech Co., Ltd. (Shanghai, China). HP1 and HP2 were heated to 90 °C for 10 min and slowly cooled to room temperature before use to form hairpin structure. The sequence of the oligonucleotides were as follows:

Hairpin DNA 1 (HP1): 5′-GACTCAGGCTTGATTAAGAGTCTTCC-3′;.

Hairpin DNA 2 (HP2): 5′-CAGGTACCTTAACGACTG CGAAGCCTGAGTC-3′;.

Target DNA: 5′-GGAAGACTCTTGTCT-3′;.

Assistance DNA: 5′-CGCAGTCGTTCTCA-3′;.

Capture probe: 5′-CGTTACGTCATGTGCTAAGGTACCTG-$(CH_2)_6$-SH-3′;.

SH-DNA: 5′-AGCACATGACGTAACG-$(CH_2)_6$-SH-3′;.

One-base mismatched DNA: 5′-GGAATACTCTTGTCT-3′;.

Two-base mismatched DNA: 5′-GGAATTCTCTTGTCT-3′;.

Noncomplementary DNA: 5′-ATCGCCAATCCAGGC-3′;.

2.2. Apparatus

Electrochemical experiments were measured with CHI 660E electrochemical workstation (CH Ins., Shanghai, China). The electrochemical detections were employed with a three-electrode system including gold electrode (GE) as working electrode, a Pt electrode as counter electrode and a saturated calomel electrode (SCE) as reference electrode. Transmission electron microscopy (TEM) images were observed with FEI Tecnai G20 transmission electron microscope (FEI company, Hillsboro, USA). UV–vis absorption spectra was recorded by UV-2700 UV–vis spectrophotometer (Shimadzu co., Ltd, Japan).

2.3. One-Step synthesis of AuNCs/GR nanohybrids

The AuNCs/GR nanohybrids were synthesized according to the method previously reported with slight modification (Yin et al., 2012). In a typical synthesis, 1.7 mg GR sheet was dissolved in 10 mL ammonia solution (pH =11, adjusted pH with 2 mM CTAB) and ultrasonically for 3 h to obtain GR solution (0.17 mg/mL). Then 100 μL $HAuCl_4$ (50 mM) was added into the above mixture and immediately ultrasonically for 10 min at room temperature with the power of 100 W. Whereafter, the obtained AuNCs/GR nanohybrids were centrifugated for 10 min at 10000 rpm and washed with ultrapure water thoroughly, then dispersed in 10 mL CTAB (2 mM).

2.4. Preparation of functionalized AuNCs/GR nanohybrids

AuNCs/GR nanohybrids were labeled with SH-DNA and ALP (AuNCs/GR-DNA-ALP) to construct the catalytic interfaces. AuNCs/GR-DNA-ALP conjugates were prepared as follows: 20 μL SH-DNA (1 μM) containing 2 mM TCEP was added into 1 mL AuNCs/GR nanohybrids and stirred for 2 h. Afterwards, 50 μL ALP (200 U/mL) with 2 μL NaOH (1 M) were introduced into the mixture and kept stirring for 3 h, and then 100 μL 1% BSA was added to blocked the unoccupied sites of AuNCs. The obtained AuNCs/GR-DNA-ALP conjugates were centrifugated for 10 min with 10000 rpm and washed with ultrapure water throughly, then dissolved in 10 mM phosphate buffer saline (PBS, pH 7.4) and stored at 4 °C for further use.

2.5. Process of Exo III-aided cascade target recycling

In the Exo III-aided cascade target recycling process, a certain concentration of target DNA was incubated with 50 μL HP1 (1 μM) containing 0.4 U/μL Exo III at 37 °C for 80 min. Then 5 μL assistance DNA (10 μM) was added into the mixture with the supplementary of 2 μL Exo III (10 U/μL). The solution was incubated for another 80 min at 37 °C to complete the Exo III-aided target recycling process. The obtained Exo III cleavage product was kept at 80 °C for 10 min to achieve the inactivation of Exo III.

2.6. Construction of the electrochemical biosensor

The bare GE was firstly polished by γ-Al_2O_3 powder and ultrasonically with ethanol and water separately, and then electrochemically cleaned by 0.5 M H_2SO_4 by cyclic voltammetry (CV) from −0.3 to 1.5 V. The bare GE was dried with nitrogen and immediately incubated with capture probe (1 μM) at room temperature overnight. Next, capture probe modified GE was dealed with MCH (1 mM) for 1 h and then incubated with the Exo III cleavage product for 1 h at 37 °C. Thereafter, the modified electrode was immersed into the prepared AuNCs/GR-DNA-ALP conjugates for 100 min. Finally, the electrode was reacted with deposition solution (pH =9.8) containing glycine (50 mM), $AgNO_3$ (1 mM) and AAP (1 mM) for 40 min in darkness.

2.7. Electrochemical measurements

Linear sweep voltammetry (LSV) was scanned in 1 M KCl solution from −0.2 V to +0.3 V with a scan rate of 100 mV/s, the electrochemical signal of the deposited AgNPs was at about +0.05 V. Amperometric i-t curves were scanned in 10 mM PBS (pH 7.4) at the potential of 150 mV with the run time of 100 s.

3. Results and discussion

3.1. Design principle of the biosensor

The multiple-amplified biosensor was constructed based on functionalized AuNCs/GR nanohybrids and Exo III-aided cascade target recycling strategy (Scheme 1). As shown in Scheme 1A, AuNCs/GR nanohybrids were labeled with SH-DNA and ALP to act as the catalytic interfaces. Exo III-aided cascade target recycling process was shown in Scheme 1B, which was initiated by target DNA. As Exo III could specifically cleave the duplex DNA from its 3′-terminus, in recycling 1, the hybridization of target DNA with HP1 led to the formation of DNA duplex, providing a suitable substrate for Exo III, which digested the formed duplex DNA, releasing target DNA and the secondary target DNA (S1). The existence of S1 and assistance DNA triggered another cleavage process of recycling 2, in which HP2 was unwrapped to form double-stranded DNA with the 3′-terminus of S1 and assistance DNA exposed. As a consequence, the formed double-stranded DNA was digested by Exo III, S1 and assistance DNA was released for new binding with HP2. The Exo III-aided cascade target recycling accomplished with the acquisition of important cleavage product (S2), which acted as linkage between the capture probe and the AuNCs/GR-DNA-ALP conjugates. In the construction of electrochemical biosensor (Scheme 1C), S2 partly hybridized with capture probe on GE and the remainder sequence hybridized with SH-DNA of the AuNCs/GR-DNA-ALP conjugates. Ultimately, AuNCs/GR-DNA-ALP conjugates catalyzed silver deposition reaction (See deposition reaction in Supporting Information). The deposited AgNPs produced a detectable electrochemical signal, which was related to the concentration of target DNA and quantified by LSV.

3.2. Characterization of the nanomaterials and modification steps of biosensor

The synthetic nanomaterials including AuNCs/GR nanohybrids, AuNCs/GR-DNA-enzyme conjugates and the deposited AgNPs on the catalytic interfaces were characterized by TEM. TEM image of AuNCs/GR nanohybrids was shown in Fig. 1A, it could be seen the spherical AuNCs were well-dispersed on the surface of GR sheets, and the size was uniform with 1.9 nm in diameter, proving the successful synthesis of AuNCs/GR nanohybrids. Fig. 1B presented the image of AuNCs/GR -DNA-ALP conjugates, it was found that the ALP absorbed on the AuNCs/GR nanohybrids. As shown in Fig. 1C, the deposited AgNPs were absorbed on the interfaces of AuNCs/GR nanohybrids, owing to the ALP-catalyzed silver deposition reaction. In addition, the functionalized AuNCs/GR nanohybrids (AuNCs/GR-DNA-enzyme conjugates) were characterized by X-ray photoelectron spectroscopy (XPS) (Thermo Fisher Scientific Lt., ESCALAB 250Xi, UK), Fourier Transform Infrared Spectroscopy (FTIR) (Perkin Elmer company, Spectrum one, USA) and Raman spectrum (Renishaw plc., Wotton-under-Edge, UK) (Fig. S1–S3). Atomic Force Microscope (AFM) (Bruker Corporation, Nanoscope IIIa, Germany) was used to characterize film thickness of the conjugates (Fig. S4) (See details in Supporting Information).

The stepwise modification process of biosensor was characterized by EIS obtained in 5 mM $[Fe(CN)_6]^{3-/4-}$ containing 0.1 M KCl with the frequency ranging from 0.1 to 10^5 Hz. The diameter of the semicircle in EIS was equivalent to charge transfer resistance (R_{ct}). Inset showed the equivalent circuit of EIS, R_S represented the electrolyte resistance, R_{ct} represented the charge transfer resistance, C_{dl} represented the double layer capacitance and Z_w represented the Warburg impedance. The value of impedance parameters was obtained by CHI 660E workstation (Table S1). In the modification process of the electrode, the R_S, C_{dl} and Z_w showed no regular change, the change of R_{ct} showed some regularity. Seen from Fig. 1D, bare GE (curve a) had the minimum R_{ct}, closing to a straight line. R_{ct} increased obviously with the modification of capture probe (curve b) and MCH (curve c), owing to oligonucleotides and MCH obstructed the electron-transfer. After hybridized with S2 (curve d) and AuNCs/GR-DNA-ALP conjugates (curve e), R_{ct} increased ulteriorly. With the completion of the modification steps, the hybridization efficiency of the conjugates was 55.0% (Jauset-Rubio et al., 2016). The enzyme-catalyzed silver deposition led the R_{ct} decreased due to the conductibility of deposited AgNPs. And the fitting curves of the modification steps in Fig. 1D were consistent with the experimental results. In addition, the corresponding CV curves were in line with that of EIS (Fig. S5).

3.3. Amplification performance of the biosensor

In order to verify the amplification performance of Exo III-aided cascade target recycling, LSV response with and without the addition of Exo III were recorded. As shown in Fig. 2A, the LSV current was inconspicuous with the absence of Exo III (curve a). However, with the presence of Exo III, LSV signal was distinct (curve b). It is mainly because of the obtained cleavage product S2 played an important role in the construction of the biosensor. Without S2, the AuNCs/GR-DNA-ALP conjugates could not hybridize with capture probe, and the ALP-catalyzed reaction could not be implemented.

To examine the catalytic effect of ALP, AuNCs/GR nanohybrids with and without ALP labeled were compared. As shown in Fig. 2B, it was found that the AuNCs/GR-DNA modified electrode had unconspicuous response (curve a), because there was no catalytic reaction happened. The AuNCs/GR-DNA-ALP conjugates modified electrode showed a distinct LSV response (curve b), owing to the ALP-catalyzed silver deposition reaction produced an amplified signal. These results indicated the ALP vastly contributed to the signal output.

The superiority of AuNCs/GR nanohybrids was examined by

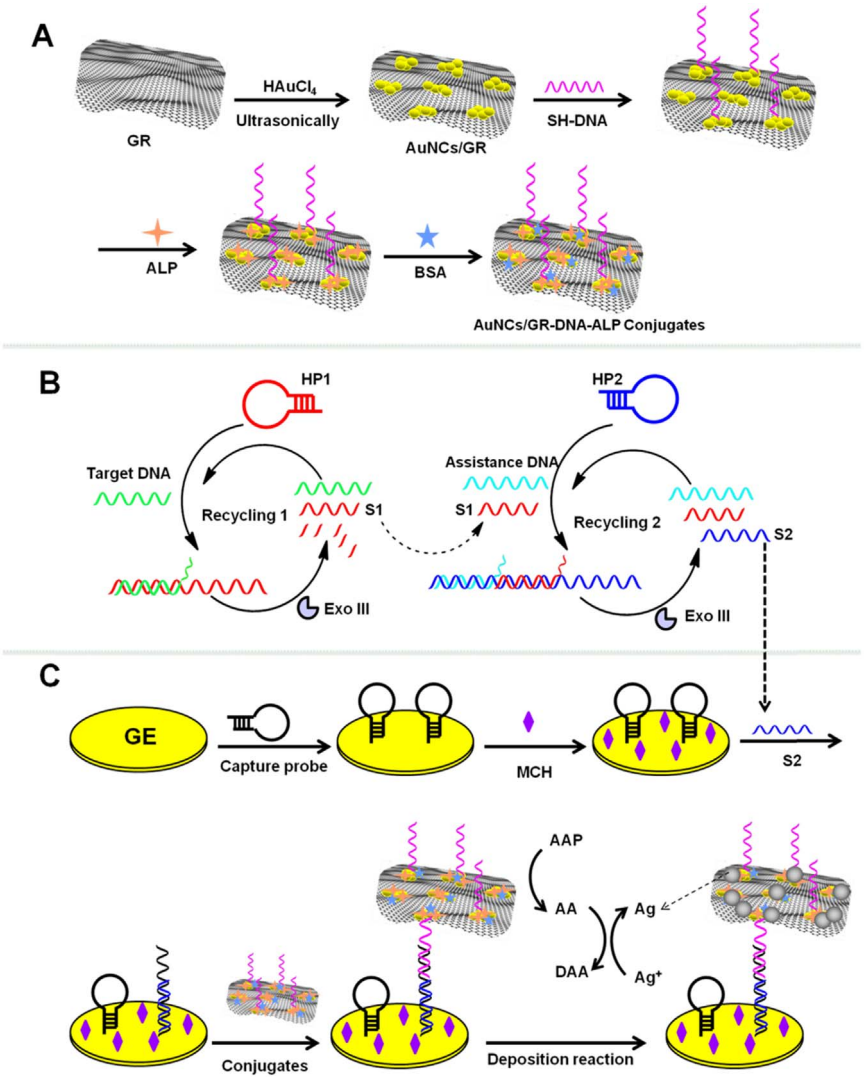

Scheme 1. Schematic Illustration of the multiple-amplified electrochemical biosensor for target DNA detection: (A) Fabrication steps of the functionalized AuNCs/GR nanohybrids; (B) Principle of the target-triggered Exo III-assisted cascade target recycling; (C) Construction of the biosensor using functionalized AuNCs/GR nanohybrids as the interfaces of enzyme-catalyzed silver deposition reaction.

compared with BSA-protected AuNCs (AuNCs@BSA). AuNCs@BSA and its conjugates were prepared (Xie et al., 2009) (Please see the synthetic procedures in Supporting Information). As shown in Fig. 2C, unimpressive LSV current was observed without modification of any conjugates (curve a). With the AuNCs@BSA-DNA-ALP conjugates hybridized on the electrode, LSV signal showed an obvious increase (curve b), due to the enzyme-catalyzed reaction. The AuNCs/GR-DNA-ALP conjugates modified electrode had the most significant signal output (curve c) compared with that of AuNCs@BSA-DNA-ALP. It is mainly because the GR as template has large specific surface area with perfect conductivity than BSA as template. These experimental results revealed the GR-templated AuNCs was superior to the protein-templated AuNCs in electrochemical performance. In addition, the purification procedure of protein-stabilized AuNCs-based conjugates usually through ultrafiltration, which is time-cost. In contrast, AuNCs/GR-based conjugates were purified by centrifugation, which was very simple and efficient.

3.4. Analytical performance of the biosensor

Under optimal experimental conditions (Optimization of the experimental conditions (Fig. S6) were presented in Supporting Information), electrochemical detection of target DNA was implemented. HP1 was incubated with a series concentration of target DNA in recycling 1, with the completion of recycling 2 and the following modification steps, LSV signals were recorded (Fig. 3A). A negligible signal was observed before the addition of target DNA (curve a), while a noticeable LSV signal was appeared at about +0.05 V with the addition of target DNA and it increased with the increasing target DNA (curve b to h). The linear calibration curve was shown in Fig. 3B, with the concentration of target DNA ranging from 0.02 fM to 20 pM, good linearity between the LSV current and logarithm of the target DNA concentration was achieved. The linear equation was fitted as $y=2.76x+13.84$ with a regression coefficient of 0.9948, Where y and x denote the LSV current intensity (μA) and the logarithm of target DNA concentration (pM), respectively. The limit of detection (LOD) was as low as 0.057 fM, which was much lower compared with different amplification strategy-based biosensor for DNA detection (Table S2). These experimental results demonstrated that this proposed biosensor could be used as an effective approach for DNA detection.

3.5. Selectivity of the biosensor

The selectivity of the biosensor for DNA detection was further investigated by examining the LSV responses towards target DNA and three different interference DNA including one-base mismatched DNA,

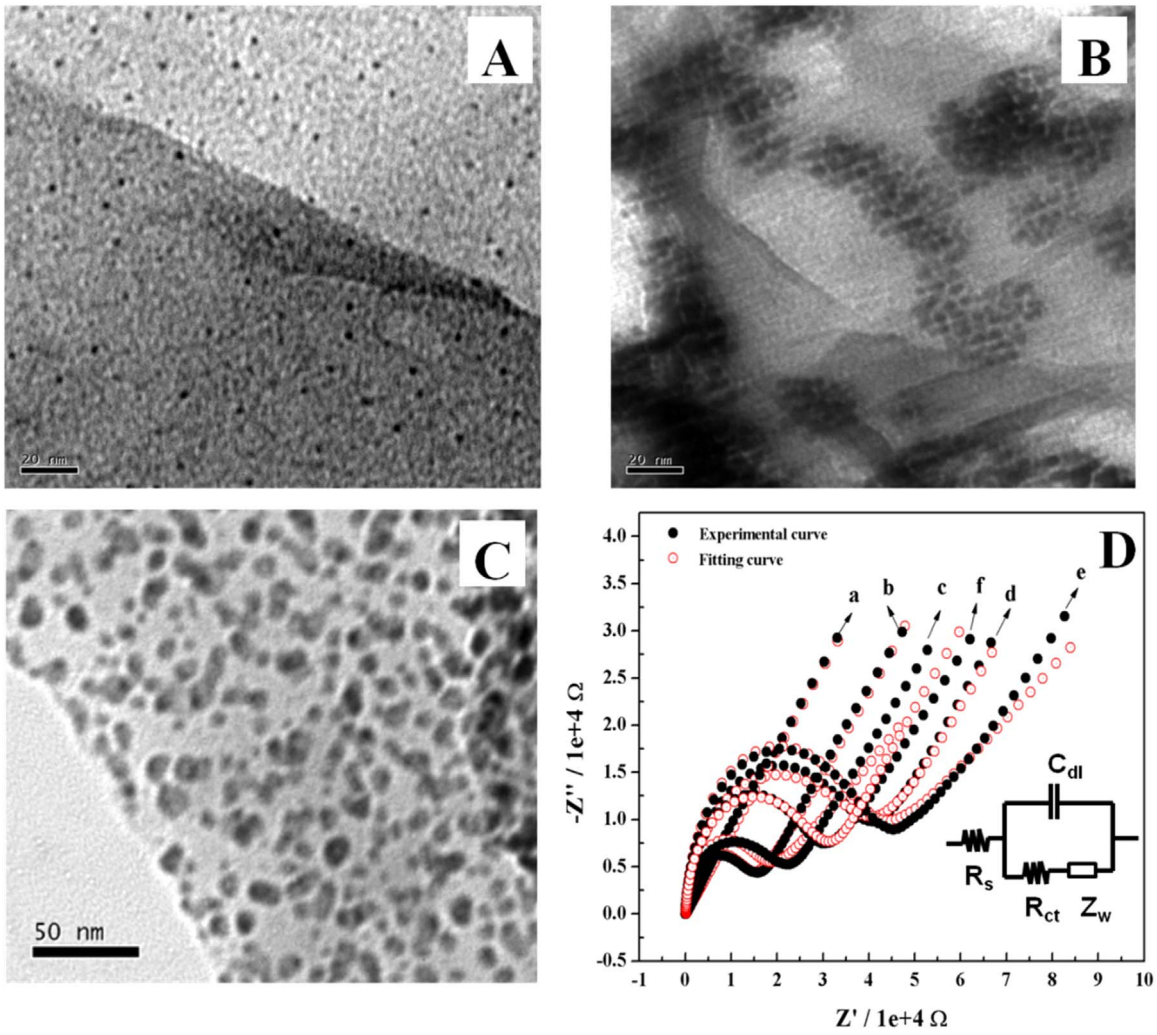

Fig. 1. TEM images of different nanomaterials: (A) AuNCs/GR nanohybrids; (B) AuNCs/GR-DNA-ALP conjugates; (C) the deposited AgNPs formed by enzyme-catalyzed silver deposition. (D) EIS plots including experimental curves and fitting curves of the modification steps of the electrochemical biosensor with 1 pM target DNA: (a) bare GE; (b) capture DNA/GE; (c) MCH/capture DNA/GE; (d) S1/MCH/capture DNA/GE; (e) S1/MCH/capture DNA/GE incubated with AuNCs/GR-DNA-ALP conjugates; (f) completion of enzyme-catalyzed silver deposition.

two-base mismatched DNA, noncomplementary DNA and without addition of any DNA (blank). As shown in Fig. S7, the addition of 0.05 pM target DNA led to remarkable signal output (column a). Nevertheless, in the presence of 1 pM one-base mismatched DNA (column b) and 1 pM two base mismatched DNA (column c), the LSV current were only about 30.8% and 17.4% of that for target DNA. The presence of 1 pM noncomplementary DNA (column d) almost had the same LSV response with the blank (column e). Therefore, the fabricated biosensor showed good selectivity for the detection of target DNA. The stability, reproducibility and repeatability of the biosensor were also investigated (See details in Supporting Information).

3.6. Detection in real samples

To validate the practical application possibility, the fabricated biosensor was used to detect target DNA in real sample. As shown in Table S3, three different concentrations of target DNA (5 pM, 0.1 pM, 0.01 pM) were added into 10-fold diluted human serum sample and detected. The recoveries were between 94.92% and 103.2%, the relative standard deviation (RSD) were between 3.4% and 5.8%, confirming the proposed biosensor obtained comparatively accurate detection results in complex biological sample with great utility.

3.7. Extension of the strategy

We also extended the type of GR-templated metal clusters rather than the type of enzyme to construct different catalytic interfaces and apply the strategy in different catalytic reaction. Herein, GR-stabilized Pt nanoclusters (PtNCs/GR) were synthesized and verified its peroxidase-like activity (The detailed synthetic procedures of PtNCs/GR nanohybrids and PtNCs/GR-DNA conjugates were presented in Supporting Information). Scheme S1 showed the fabrication process of the biosensor based on functionalized PtNCs/GR nanohybrids which catalyzed the TMB-H_2O_2 system to produce an electrochemical signal.

The peroxidase-like activity of PtNCs/GR nanohybrids were verified by catalyzing the peroxidase substrate TMB in the presence of H_2O_2 (Josephy et al., 1982). 50 μL PtNCs/GR nanohybrids were added into 1 mL TMB-H_2O_2 system (0.25 mM TMB and 20 mM H_2O_2), the UV–vis spectra was recorded with the wavelength ranging from 500 nm to 800 nm. As shown in Fig. 4A, there was scarcely any absorption without PtNCs/GR nanohybrids (curve a), indicating no oxidative reaction of TMB happened. However, with the presence of PtNCs/GR nanohybrids, a strong absorption peak appeared at 652 nm (curve b), manifesting the catalytic activity of PtNCs/GR nanohybrids towards TMB-H_2O_2 system. The inset of Fig. 4A displayed the picture of the solution in the absence and presence of PtNCs/GR nanohybrids in the TMB-H_2O_2 mixture. The TMB- H_2O_2 solution was colorless (a) without

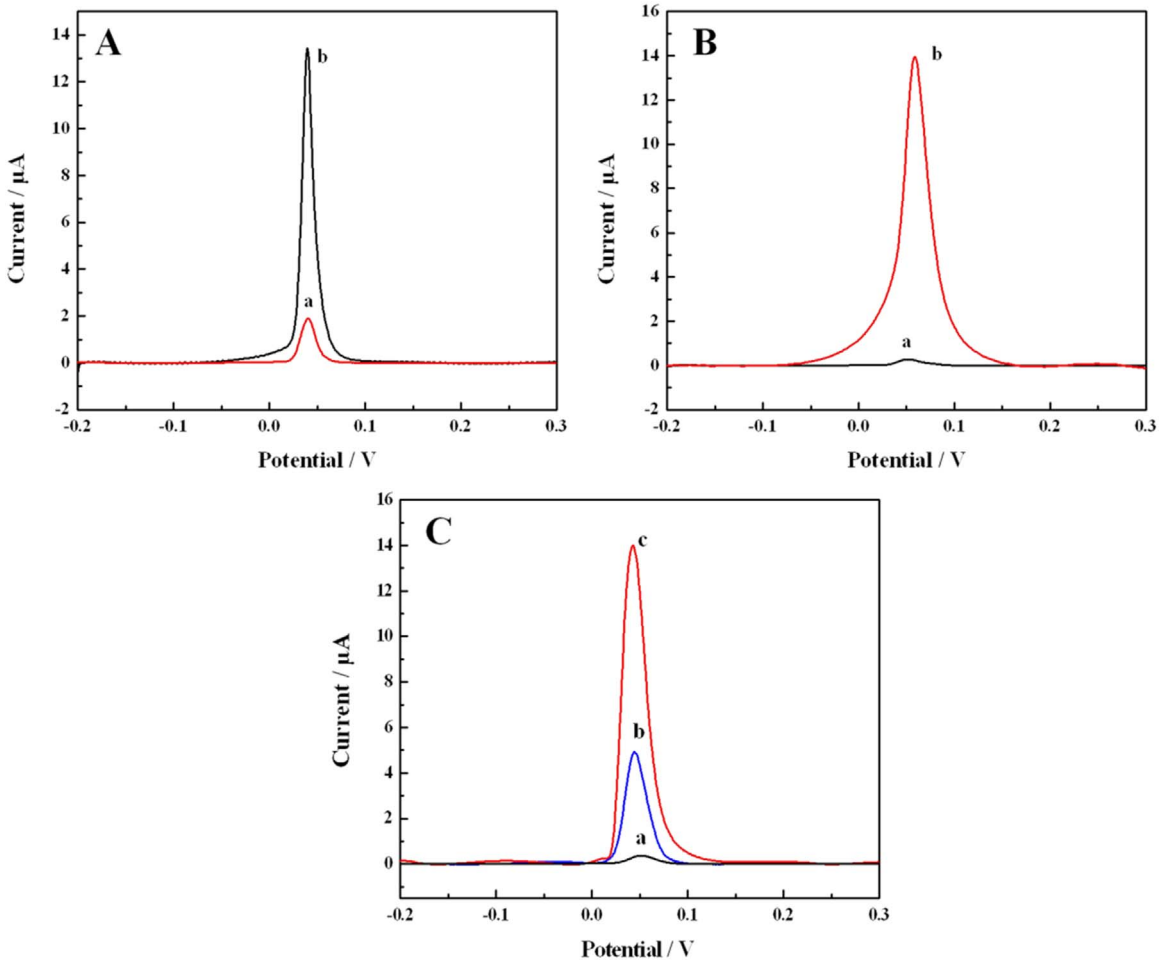

Fig. 2. Capture probe modified electrodes of (A) LSV response of in the absence (a) and presence (b) of Exo-III; (B) LSV signal with and without the addition of ALP: (a) AuNCs/GR-DNA conjugates; (b) AuNCs/GR-DNA-ALP conjugates (C) Comparison of catalytic performance of the AuNCs/GR-based and AuNCs@BSA-based conjugates: (a) without any conjugates; (b) AuNCs@BSA-DNA-ALP conjugates; (c) AuNCs/GR-DNA-ALP conjugates. All electrodes were finally performed with the silver deposition reaction to produce LSV signal.

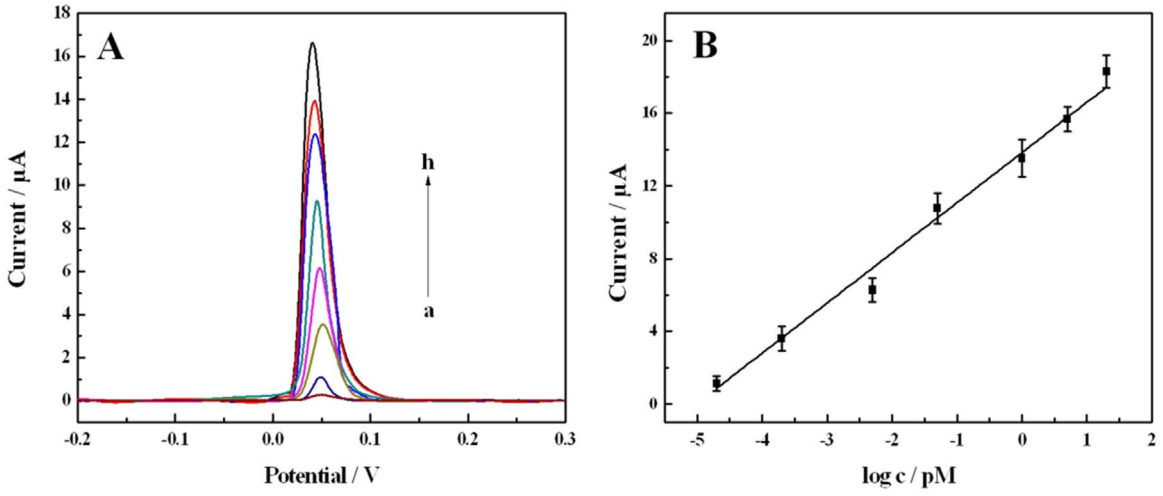

Fig. 3. (A) LSV responses corresponding to different concentrations of target DNA: (a) 0, (b) 0.02 fM, (c) 0.2 fM, (d) 5 fM, (e) 0.05 pM, (f) 1 pM, (g) 5 pM, (h) 20 pM. (B) Linear relationship between LSV current and the logarithm concentration of target DNA ranging from 0.02 fM to 20 pM.

PtNCs/GR nanohybrids, while the color became blue (b) with the addition of PtNCs/GR nanohybrids, which were in consistent with the spectrum results. These experimental results revealed the peroxidase-like activity of the PtNCs/GR nanohybrids.

In order to test the catalytic performance of the constructed biosensor, well-prepared electrodes were used to detect in 10 mM PBS (pH 7.4) containing 0.25 mM TMB and 20 mM H_2O_2, and the amperometric i-t curves were recorded. As shown in Fig. 4B, in the absence of target DNA, the amperometric response was unobvious (curve a), indicating the catalytic reaction did not occur. With the presence of target DNA, the amperometric signal increased significantly (curve b), because of the cleavage product (S2) linked the

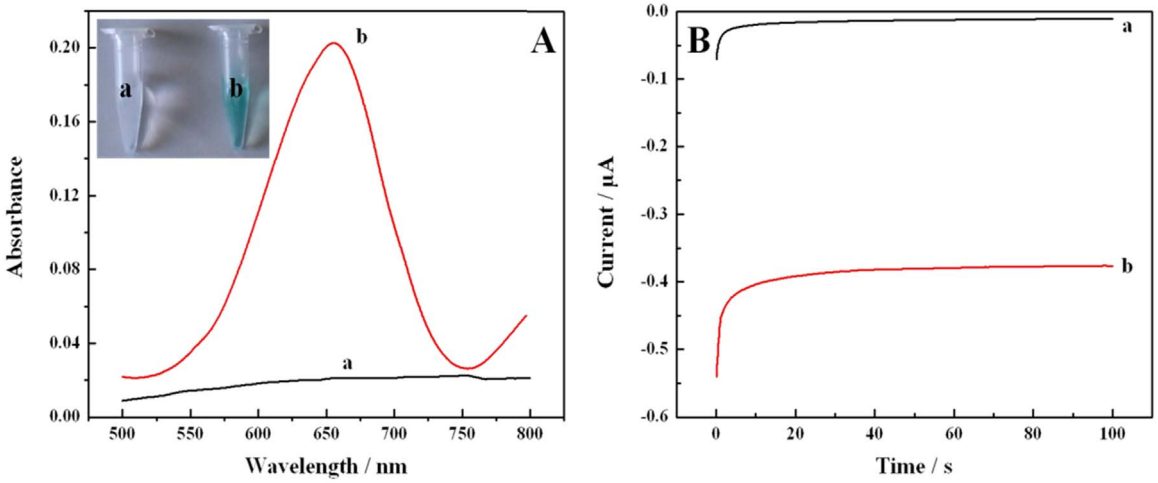

Fig. 4. (A) UV–vis absorption spectra of 1 mL mixture solution containing 0.25 mM TMB and 20 mM H_2O_2 in the absence (a) and presence (b) of 50 μL synthesized PtNCs/GR nanohybrids. Inset : Pictures of corresponding mixture solution without (a) and with (b) the addition of PtNCs/GR nanohybrids under natural light. (B) Amperometric responses of the proposed electrochemical biosensor in 10 mM PBS containing 0.25 mM TMB and 20 mM H_2O_2: (a) no target DNA; (b) 1 pM target DNA.

capture DNA and the PtNCs/GR-DNA conjugates, leading to the oxidation of TMB with the existence of H_2O_2. Therefore, the PtNCs/GR-based catalytic interfaces were successfully applied into the detection of DNA. As a consequence, by changing the type of GR-templated metal nanoclusters, different catalytic interfaces also could be constructed and applied in different catalytic reactions.

4. Conclusions

In summary, a novel and ultrasensitive electrochemical biosensor for DNA detection was developed using AuNCs/GR nanohybrids-based catalytic interfaces and Exo III-aided cascade target recycling amplification strategy. The cleavage product of Exo III-aided cascade target recycling and enzyme labeled AuNCs/GR nanohybrids collectively constructed the catalytic interfaces of the biosensor. By taking advantage of the multiple amplification strategy, ultrasensitive and selective detection of target DNA was achieved with a detection limit of 0.057 fM. In addition, by utilizing the potential of GR as the universal template to synthesize different metal nanoclusters, such as PtNCs/GR, different catalytic interfaces and reactions could be achieved. Therefore, this strategy held great promise as an effective method for DNA detection and showed great potential in early diagnosis of gene-related diseases.

Acknowledgments

This work was supported by the National Natural Science Foundation of China (Grant No. 21475032, 21405035).

Appendix A. Supporting information

Supplementary data associated with this article can be found in the online version at doi:10.1016/j.bios.2016.12.017.

References

Bao, T., Wen, W., Zhang, X.H., Xia, Q.H., Wang, S.F., 2015. Biosens. Bioelectron. 70, 318–323.
Basnar, B., Weizmann, Y., Cheglakov, Z., Willner, I., 2006. Adv. Mater. 18, 713–718.
Chang, H.-C., Ho, J.-A.A., 2015. Anal. Chem. 87, 10362–10367.
Chargaff, E., 1951. Fed. Proc. 10, 654–659.
Chen, M., Hou, C.J., Huo, D.Q., Bao, J., Fa, H.B., Shen, C.H., 2016. Biosens. Bioelectron. 85, 684–691.
Ding, H., Liang, C.S., Sun, K.B., Wang, H., Hiltunen, J.K., Chen, Z.J., Shen, J.C., 2014. Biosens. Bioelectron. 59, 216–220.
Farrag, M., Tschurl, M., Heiz, U., 2013. Chem. Mater. 25, 862–870.
Feng, K.J., Zhao, J.J., Wu, Z.-S., Jiang, J.H., Shen, G.L., Yu, R.Q., 2011. Biosens. Bioelectron. 26, 3187–3191.
Fu, Y.-H., Pizzuti, A., Fenwick, R.G., King, J.J., Rajnarayan, S., Dunne, P.W., Dubel, J., Nasser, G.A., Ashizawa, T., Jong, P., Wineringa, B., Korneluk, R., Perryman, M.B., Epstein, H.F., Caskey, C.T., 1992. Science 255, 1256-1258.
Gerasimova, Y.V., Kolpashchikov, D.M., 2014. Chem. Soc. Rev. 43, 6405–6438.
Holzer, P., 1998. Digestion 59, 269–283.
Huang, H.Y., Bai, W.Q., Dong, C.X., Guo, R., Liu, Z.H., 2015. Biosens. Bioelectron. 68, 442–446.
Jauset-Rubio, M., Svobodová, M., Mairal, T., McNeil, C., Keegan, N., El-Shahawi, M.S., Bashammakh, A.S., Alyoubi, A.O., O'Sullivan, C.K., 2016. Anal. Chem. 88, 10701–10709.
Jin, R.C., 2015. Nanoscale 7, 1549–1565.
Josephy, P., Eling, T., Mason, R., 1982. J. Biol. Chem. 257, 3669–3675.
Kaghad, M., Bonnet, H., Yang, A., Creancier, L., Biscan, J.-C., Valent, Alexandre, Minty, A., Chalon, P., Lelias, J.-M., Dumont, X., Ferrara, P., McKeon, F., Caput, D., 1997. Cell 90, 809–819.
Kawasaki, H., Yamamoto, H., Fujimori, H., Arakawa, R., Iwasaki, Y., Inada, M., 2010. Langmuir 26, 5926–5933.
Levinson, B., Janco, R., Phillips, J., Gitschier, J., 1987. Nucl. Acids Res. 15, 9797–9805.
Liu, P., Yang, X.H., Sun, S., Wang, Q., Wang, K., Huang, J., Liu, J.B., He, L.L., 2013. Anal. Chem. 85, 7689–7695.
Liu, S.F., Wei, W.J., Wang, Y.Q., Fang, L., Wang, L., Li, F., 2016. Biosen. Bioelectron. 80, 208–214.
Liu, S.F., Cheng, C.B., Liu, T., Wang, L., Gong, H.W., Li, F., 2015. Biosen. Bioelectron. 63, 99–104.
Liu, X.F., Li, C.H., Xu, J.L., Lv, J., Zhu, M., Guo, Y.B., Cui, S., Liu, H.B., Wang, S., Li, Y.L.J., 2008. Phys. Chem. C 112, 10778–10783.
Ngo, H.T., Gandra, N., Fales, A.M., Taylor, S.M., Vo-Dinh, T., 2016. Biosens. Bioelectron. 81, 8–14.
Rosi, N.L., Giljohann, D.A., Thaxton, C.S., Lytton-Jean, A.K.R., Han, M.S., Mirkin, C.A., 2006. Science 312, 1027–1030.
Shamsipur, M., Farzin, L., Tabrizi, M.A., Molaabasi, F., 2015. Biosens. Bioelectron. 74, 369–375.
Sun, J., Yang, F., Zhao, D., Yang, X.R., 2014. Anal. Chem. 86, 7883–7889.
Tan, Y., Wei, X.F., Zhao, M.M., Qiu, B., Guo, L.H., Lin, Z.Y., Yang, H.-H., 2015. Anal. Chem. 87, 9204–9208.
Venkatesh, V., Shukla, A., Sivakumar, S., Verma, S., 2014. ACS Appl. Mater. Inter. 6, 2185–2191.
Wang, T., Zhou, L.L., Bai, S.L., Zhang, Z., Li, J.L., Jing, X.Y., Xie, G.M., 2016. Biosens. Bioelectron. 78, 464–470.
Wang, Y.J., Bai, X.N., Wen, W., Zhang, X.H., Wang, S.F., 2015. ACS Appl. Mater. Inter 7, 18872–18879.
Xie, J.P., Zheng, Y.G., Ying, J.Y., 2009. J. Am. Chem. Soc. 131, 888–889.
Xiong, E.H., Yan, X.X., Zhang, X.H., Liu, Y.Q., Zhou, J.W., Chen, J.H., 2017. Biosens. Bioelectron. 87, 732–736.
Ye, Y.D., Xia, L., Xu, D.D., Xing, X.J., Pang, D.W., Tang, H.W., 2016. Biosens. Bioelectron. 85, 837–843.
Yin, H.J., Tang, H.J., Wang, D., Gao, Y., Tang, Z.Y., 2012. ACS Nano 6, 8288–8297.
Yun, W., Jiang, J., Cai, D., Zhao, P., Liao, J., Sang, G., 2016. Biosens. Bioelectron. 77, 421–427.
Zeng, Z., Liu, Y., Wei, J., 2016. TrAC-Trend Anal. Chem. 75, 162–173.
Zhang, H.Q., Li, F., Dever, B., Li, X.-F., Le, X.C., 2013. Chem. Rev. 113, 2812–2841.
Zhang, M., Guan, Y.-M., Ye, B.-C., 2011. Chem. Commun. 47, 3478–3480.
Zhao, Y.X., Chen, F., Li, Q., Wang, L.H., Fan, C.H., 2015. Chem. Rev. 115, 12491–12545.
Zuo, X.L., Xia, F., Xiao, Y., Plaxco, K.W., 2010. J. Am. Chem. Soc. 132, 1816–1818.